Coral Reefs (2013) 32:293–303
DOI 10.1007/s00338-012-0982-0

REPORT

An abrupt backreef infilling in a Holocene reef, Paraoir, Northwestern Luzon, Philippines

Shou-Yeh Gong · Tso-Ren Wu · Fernando P. Siringan · Ke Lin · Chuan-Chou Shen

Received: 20 June 2012 / Accepted: 1 November 2012 / Published online: 19 November 2012

Abstract We describe a sudden backreef infilling at the west coast of Luzon, Philippines, which occurred after 324 ± 12 yr ago (year BP, before 1950 AD). Results of 30 ^{230}Th-dated fossil corals from the surface and 5 cores, 17–29.1 m in length, recovered from a Holocene reef at Paraoir show that the reef flat developed in two stages. The reef margin is dated at 10,256 ± 50 (2σ) yr BP at 23.9 m below mean sea level (MSL) and about 6,654 ± 29 yr BP at 3.7 m below MSL with ages increasing with depth. The reef flat was formed with sediments of 818–324 yr BP old, which do not follow an age–depth correlation. The evidence suggests that a backreef moat remained empty throughout the buildup of the reef for about 6 kyr and was filled abruptly with a 26-m-thick succession of rubble and bioclastics by an extreme wave event (EWE) after 324 ± 12 yr BP. Field evidence, historical records, and tsunami simulation suggest the EWE sedimentation was likely caused by a single severe tropical cyclone, although the possibility of tsunami is not ruled out. The Paraoir reef flat was built up in a mode different from previously reported cases of Holocene reefs.

Keywords Holocene reef · Backreef infilling · Extreme wave event · Tropical cyclone · Philippines · Coral U–Th dating

Communicated by Geology Editor Prof. Bernhard Riegl

S.-Y. Gong
Department of Geology, National Museum of Natural Science, Taichung 40419, Taiwan, ROC

T.-R. Wu
Institute of Hydrological and Oceanic Sciences, National Central University, Jhongli City 32001, Taiwan, ROC

F. P. Siringan
Marine Science Institute, University of Philippines, 1101 Quezon City, Philippines

K. Lin · C.-C. Shen (✉)
High-Precision Mass Spectrometry and Environment Change Laboratory (HISPEC), Department of Geosciences, National Taiwan University, No. 1, Sec. 4, Roosevelt Road, Taipei 10617, Taiwan, ROC
e-mail: river@ntu.edu.tw

Introduction

The relationship between reef framework growth and backreef infilling in Holocene reefs is complicated (Kennedy and Woodroffe 2002; Montaggioni 2005; Purdy and Gischler 2005). The classic view is that the balance between reef growth and backreef deposition is primarily controlled by sea level changes and growth rates along the reef margin, and lagoons will remain unfilled as empty buckets (Schlager 1993; Yamano 2000; Purdy and Gischler 2005). Most case studies show that a reef crest mainly was initiated by coral growth in the early Holocene and reached present levels in association with a Mid-Holocene highstand (Yamano 2000; Kennedy and Woodroffe 2002; Montaggioni 2005), while backreef areas are filled by bioclastic deposits when sea level stabilized after 6000 yr BP (relative to 1950 AD) and mostly remain unfilled (Schlager 1993; Purdy and Gischler 2005; Hopley et al. 2007). Purdy and Gischler (2005) further pointed out that this "empty bucket" is only temporary status. Nevertheless, backreef filling is considered a process that will take at least several thousand years (Smith et al. 1998; Cabioch et al. 1999; Yamano et al. 2001; Kayanne et al. 2002; Kennedy and Woodroffe 2000; Purdy and Gischler 2005). In the last couple of decades, studies have shown that in

addition to sea level changes, severe storms play an important role in redistributing sediments from reef margins landward and accelerating the process of backreef infilling in fringing reefs (e.g., Hubbard 1992; Scoffin 1993; Blanchon et al. 1997; Braithwaite et al. 2000; Macintyre et al. 2001; Yamano et al. 2001; Rasser and Riegl 2002).

In this paper, we describe a Holocene backreef infilling at Paraoir, La Union Province, Philippines, in which a 26-m-thick section of sediments were deposited by an extreme wave event (EWE) and the reef flat was built up abruptly. To our knowledge, such a sudden reef-flat buildup has not been reported before. We present lithofacies, ^{230}Th age data, historical archives of seventeenth–nineteenth centuries, and tsunami simulation to document the backreef deposition at Paraoir and propose that the EWE at Paraoir was probably caused by a severe tropical cyclone after 324 ± 12 yr BP.

Study area

Paraoir is located at 16°48′N, 120°19′E on the coast of La Union, Luzon, facing the South China Sea (Fig. 1a). The La Union and adjacent provinces are known for the occurrence of Holocene raised reefs (Maeda and Siringan 2004; Ramos and Tsutsuni 2010). Tides in the area are mixed diurnal and semidiurnal types with an average tidal range of 0.64 m (NAMRIA 2001). The dry season is from November to April and the wet season falls during the other months. Annual rainfall is about 2,400 mm and annual average temperature 25.8 °C.

Modern coral reefs occur extensively along the La Union coasts from Luna, just north of Paraoir, St Fernando City, Bauang, all the way to the Lingayen Peninsula (Aliño et al., 2003). Holocene reefs crop out at Paraoir coast, extending about 700 m along the coast, and 150–200 m perpendicular to the coast. The reef is attached to the land in the south and has a backreef moat in the northern part (Fig. 1b). The top of the reef flat was slightly truncated by wave erosion and currently exhibits three elevation levels. The highest level is represented by a coral rubble rampart occurring only in the northern part with a height of 2.4 m above mean sea level (MSL) (as shown in dark gray area in Fig. 1b). The rampart is already stabilized by partial cementation and vegetation. The second level includes most of the inner flat that is 0.3–0.5 m above MSL and about 100–150 m wide perpendicular to the coast (as shown in light gray area in Fig. 1b). The surface is already lithified as hard rock, with centimeter-scale karst developed on the surface. Head corals exposed on the surface are mostly truncated at their tops, indicating the surface has been leveled by wave erosion (Fig. 2a). Branch coral shingles are also common on the surface and tend to be less cemented. The representative corals on the surface are *Acropora, Pocillopora, Porites,* and *Platygyra*. Spurs and grooves, presumably originating during the Holocene, are well preserved. Coral rubble is commonly observed on the groove cliff (Fig. 2b). The lowest level includes the margin of the Holocene reef and the southern part the reef flat (as enclosed by a thin line without shade in Fig. 1b); it is just below MSL, only barely exposed during lower low tides. The surface is covered by seaweed or exposed rock. Living *Pocillopora verrucosa* thrives along the reef edge.

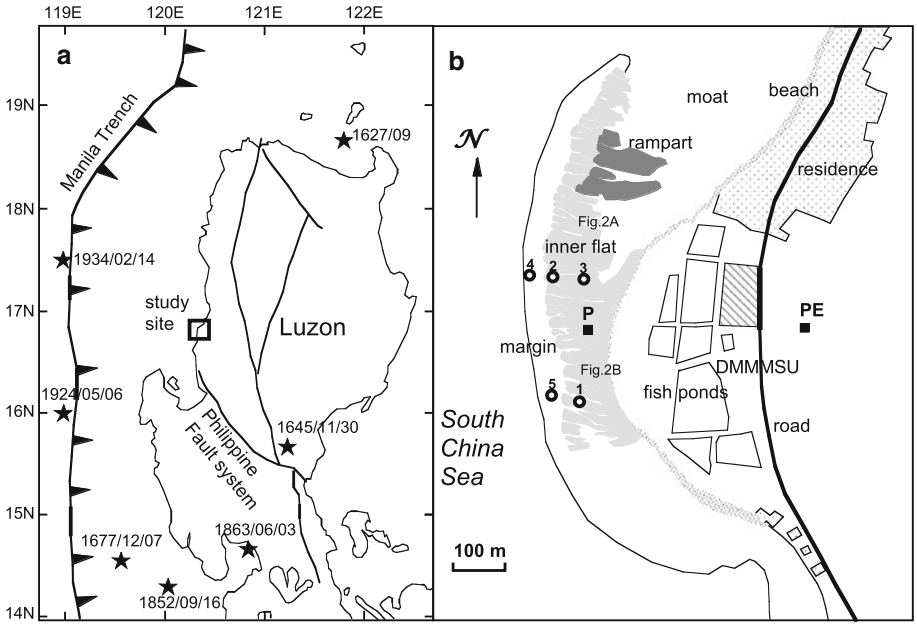

Fig. 1 **a** Geodynamic setting of Luzon, location of the study site, and estimated epicenter of tsunamigenic earthquakes of the seventeenth to nineteenth centuries (*stars*, Bautista and Oike 2000). **b** Map of the study area with elevation levels and core locations. The area bounded by a *thin line number 1–5* denotes to core PAR-1 to PAR-5. Location of Fig. 2a and b is shown on the map. The virtual wave gauges used in the earthquake-induced tsunami simulation are marked by *solid squares*, labeled with *P* and *PE*. The third gauge, *PW*, not shown in the map, is 800 m westward from *P*

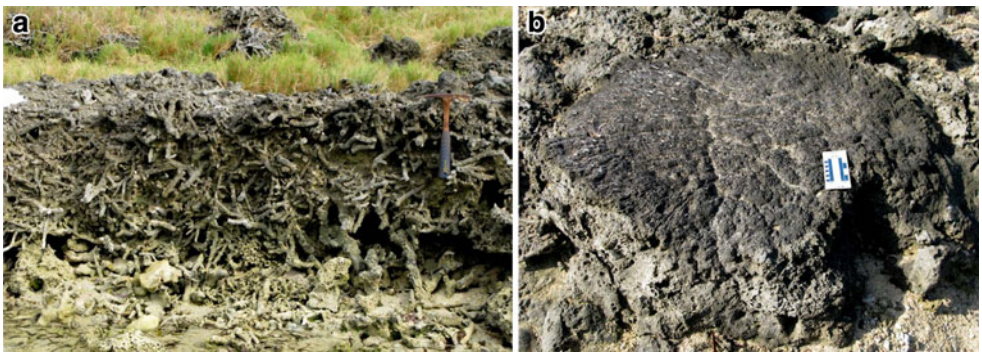

Fig. 2 Photographs of outcrops of the Paraoir reef. **a** Coral rubble on cliff of grooves on inner flat. **b** Head coral *Platygyra* on the inner flat was truncated on *top*

Materials and methods

We recovered five cores, each 6.1 cm in diameter. These cores are aligned along two East–West profiles. Their locations, wellhead elevations, and depths are provided in Figs. 1 and 4. Cores were split, photographed, and described.

A total of 30 fossil corals, including three from the surface near PAR-1 and 1 from the rampart were selected for U–Th dating. Detailed U–Th chemistry, instrumental isotopic analysis, and ^{230}Th age calculations were described in previous studies (Shen et al. 2002, 2003, 2008, 2012). The absence of secondary carbonates in the intraskeletal structure, the ^{238}U levels of 2.3–4.7 ppm, and the initial δ^{234}U values of 139.6–146.8 ‰ as in modern corals suggest that the coral samples are well preserved. Agreement of replicated ^{230}Th dates (IDs of replicated dates for coeval samples are given as "PAR-xxx–R" in Table 1) also confirms our U–Th methodology and sample quality.

Historical archives of typhoons and tsunamis of Philippines from seventeenth to eighteenth centuries were provided by Spanish missionaries during colonial time and compiled by Selga (1935), Saderra Masó (1910), and Repetti (1946).

Earthquake-induced tsunami simulation was conducted following the assumption of Liu et al. (2009) and using the widely validated Cornell Multi-grid Coupled Tsunami (COMCOT) model that solves the linear shallow water equations in a spherical coordinate system using a finite difference algorithm and the leap-frog scheme (Liu et al. 1994; Wang and Liu 2006; Wu et al. 2008; Wu and Huang 2009; Megawati et al. 2009). The computation is carried out on a 0.5-min grid extending from 118.5 E to 122.5 E, and from 13.5 N to 19.5 N. Both Coriolis force and Manning bottom friction force are considered. Conventional radiation boundary conditions are applied to each domain border. The simulations are preceded in a regional field determined by scaling law proposed by Yen and Ma (2011) to derive values of the fault parameters for the 1934 tsunami as: Mw 7.9, length of rupture 82.6 km, width 35.9 km, slip 2.9 m, strike (φ) 338°, dip (δ) 46°, rake (λ) 53°, depth to top of fault 10 km. Half-space homogenous elastic mode (Okada 1986) is adopted to generate the initial tsunami profile. In order to observe the free-surface elevation temporally, we install three virtual wave gauges, PW, P, and PE, to estimate the largest wave heights (Figs. 1b, 6).

Results

Lithology

Five lithofacies are recognized on the basis of constituents and texture: (1) boundstone facies, (2) boundstone with clayey matrix facies, (3) coral rubble facies, (4) coral rubble with clayey matrix facies, and (5) volcanic and bioclastic facies.

The boundstone facies consists of algal–coral boundstones, with some corals partially coated by microbial cements (Fig. 3a). The representative coral species are robust *Acropora* and *Porites*. The facies occurs in the upper part of cores PAR-4 and PAR-5 (Fig. 4) that are located along the reef margin and is interpreted to represent the reef framework. The boundstone with clayey matrix facies is composed of algal–coral boundstone but with a soft clayey matrix. The facies only occurs as short intervals in the middle of cores PAR-4.

The coral rubble facies comprises coral rubble of several centimeters up to several tens of centimeters and finer bioclastics (Fig. 3b). The sediments are better cemented toward the surface and remain loose or little cemented at greater depth. Some rubble are partly coated by calcareous red algae and some by microbial cements but not bounded together as framework. This facies occurs in the upper and middle parts of PAR-1, 2, and 3 (Fig. 4). The coral rubble with clayey matrix facies is similar to the coral rubble facies but with a soft clayey matrix. This facies mostly

Table 1 U–Th isotopic compositions and ^{230}Th ages for fossil coral samples of Paraoir, Philippines, by MC-ICPMS

Sample ID	Depth (m)	^{238}U (ppb)	^{232}Th (ppt)	δ^{234}U measured[a]	[^{230}Th/^{238}U] activity[b]	[^{230}Th/^{232}Th] (ppm)[c]	Age uncorrected	Age (yr BP) corrected[b,d]	$\delta^{234}U_{initial}$ corrected[e]
PAR-1 A	+0.5	2,353.3 ± 3.8	408.8 ± 5.0	145.7 ± 2.4	0.007662 ± 0.000083	729 ± 12	732.6 ± 8.1	669.6 ± 9.1	146.0 ± 2.4
PAR-1 2.9 m	−2.5	2,340.8 ± 2.4	928.9 ± 13	144.0 ± 1.9	0.00714 ± 0.00081	297 ± 34	684 ± 78	615 ± 79	144.3 ± 1.9
PAR-1 5.9 m	−5.5	2,415.6 ± 3.9	397.6 ± 9.1	145.7 ± 3.6	0.00761 ± 0.00019	764 ± 26	728 ± 18	665 ± 19	146.0 ± 3.6
PAR-1 5.9 m-R	−5.5	2,417.8 ± 2.7	1,123 ± 12	145.6 ± 2.0	0.00723 ± 0.00044	257 ± 16	692 ± 42	622 ± 44	145.9 ± 2.0
PAR-1 9.1 m	−8.7	2,950.8 ± 4.8	112 ± 13	142.8 ± 2.5	0.00603 ± 0.00027	2,624 ± 328	578 ± 26	518 ± 26	143.0 ± 2.5
PAR-1 12.7 m	−12.3	2,054.1 ± 2.3	9.6 ± 4.0	142.4 ± 2.0	0.00898 ± 0.00024	31,833 ± 13,265	862 ± 23	803 ± 23	142.7 ± 2.0
PAR-1 15.1 m	−14.7	2,263.9 ± 2.9	2,212 ± 12	144.0 ± 2.1	0.00692 ± 0.00037	116.9 ± 6.3	662 ± 36	580 ± 42	144.2 ± 2.1
PAR-1B	+0.4	2,523.3 ± 5.2	50.2 ± 5.3	145.1 ± 3.1	0.007900 ± 0.000088	6,553 ± 693	755.8 ± 8.7	696.4 ± 8.7	145.4 ± 3.1
PAR-1B-R	+0.4	2,329.5 ± 2.8	79 ± 12	145.7 ± 2.0	0.00784 ± 0.00030	3,799 ± 587	749 ± 28	689 ± 28	146.1 ± 2.0
PAR-1C	+0.4	2,408.8 ± 6.3	52.5 ± 4.0	146.6 ± 3.8	0.006649 ± 0.000079	5,037 ± 388	635.0 ± 7.8	675.5 ± 7.8	146.9 ± 3.8
PAR-1C-R	+0.4	2,683.3 ± 4.2	38 ± 10	146.3 ± 2.5	0.00642 ± 0.00023	7,391 ± 1,984	613 ± 22	554 ± 22	146.6 ± 2.5
PAR-2 3.3 m	−2.9	2,308.7 ± 6.1	1,986 ± 10	146.0 ± 3.6	0.00724 ± 0.00020	138.9 ± 3.9	692 ± 20	613 ± 28	146.3 ± 3.6
PAR-2 5.3 m	−4.9	2,549.9 ± 4.6	49.2 ± 7.2	143.4 ± 2.7	0.00732 ± 0.00021	6,257 ± 928	701 ± 20	642 ± 20	143.7 ± 2.7
PAR-2 9.3 m	−8.9	2,648.3 ± 4.4	323.5 ± 7.9	141.8 ± 2.6	0.00756 ± 0.00064	1,021 ± 90	725 ± 62	663 ± 62	142.1 ± 2.6
PAR-2 18.5 m	−18.1	3,304.8 ± 4.8	107.9 ± 6.6	139.6 ± 2.3	0.00452 ± 0.00026	2,286 ± 191	434 ± 25	374 ± 25	139.7 ± 2.3
PAR-2 25.7 m	−25.3	2,789.6 ± 4.2	1,376.3 ± 8.0	141.6 ± 2.4	0.00675 ± 0.00027	226.0 ± 9.1	648 ± 26	577 ± 28	141.9 ± 2.4
PAR-2 25.7 m-R	−25.3	2,511.9 ± 7.5	1,341 ± 14	139.6 ± 4.5	0.00650 ± 0.00027	200.9 ± 8.5	624 ± 26	553 ± 29	139.9 ± 4.5
PAR-3 0.4 m	0	2,545.7 ± 8.7	1,110 ± 13	141.0 ± 5.0	0.00602 ± 0.00019	228.2 ± 7.6	578 ± 18	509 ± 21	141.2 ± 5.0
PAR-3 0.4 m-R	0	2,790.5 ± 3.0	296 ± 13	146.8 ± 1.8	0.00650 ± 0.00042	1,012 ± 80	621 ± 41	559 ± 41	147.0 ± 1.9
PAR-3 2.9 m	−2.5	2,437.3 ± 6.1	927.4 ± 8.5	144.4 ± 3.8	0.00694 ± 0.00019	301.3 ± 8.8	665 ± 19	597 ± 21	144.7 ± 3.8
PAR-3 9.8 m	−9.4	2,870.4 ± 4.7	927 ± 13	144.5 ± 2.8	0.00615 ± 0.00018	315 ± 10	589 ± 17	522 ± 18	144.8 ± 2.8
PAR-3 12.5 m	−12.1	3,050.9 ± 4.0	419.2 ± 12	143.6 ± 2.2	0.00612 ± 0.00020	735 ± 33	586 ± 20	524 ± 20	143.9 ± 2.2
PAR-3 15.4 m	−15.0	3,803 ± 10	763.4 ± 7.0	145.5 ± 4.0	0.00406 ± 0.00012	334 ± 10	388 ± 11	324 ± 12	145.7 ± 4.0
PAR-3 15.4 m-R	−15.0	4,731.5 ± 5.5	1,348 ± 13	143.0 ± 1.9	0.00401 ± 0.00017	232 ± 10	383 ± 16	318 ± 17	143.1 ± 1.9
Rampart-2	+1.5	2,035.9 ± 6.1	16.6 ± 4.7	144.4 ± 4.5	0.00854 ± 0.00011	17,331 ± 4,951	818 ± 11	759 ± 11	144.8 ± 4.5
Paraoir4-4.4 m	−4.4	2,651.8 ± 3.2	130.7 ± 5.7	145.3 ± 2.0	0.07301 ± 0.00018	24,462 ± 1,078	7,184 ± 23	7,122 ± 23	148.3 ± 2.1
Paraoir4–7 m	−7.0	2,712.8 ± 4.2	672.6 ± 7.1	145.3 ± 2.2	0.07874 ± 0.00018	5,243 ± 56	7,766 ± 24	7,701 ± 24	148.5 ± 2.3
Paraoir4–15.2 m	−15.2	2,937.0 ± 9.0	508.4 ± 4.9	142.6 ± 4.7	0.09195 ± 0.00041	8,771 ± 89	9,146 ± 59	9,082 ± 59	146.3 ± 4.9
Paraoir4–17.5 m	−17.5	3,293.6 ± 5.0	340 ± 10	143.3 ± 2.2	0.09471 ± 0.00024	15,163 ± 448	9,426 ± 32	9,364 ± 32	147.2 ± 2.3
Paraoir4–20 m	−20.0	3,249.2 ± 5.7	1,109 ± 14	145.7 ± 2.6	0.09875 ± 0.00026	4,777 ± 62	9,824 ± 36	9,756 ± 36	149.8 ± 2.6
Paraoir4–23.6 m	−23.6	2,964.8 ± 3.6	250 ± 12	143.9 ± 2.1	0.10266 ± 0.00039	20,123 ± 1,005	10,249 ± 46	10,187 ± 46	148.1 ± 2.2
Paraoir4–23.9 m	−23.9	2,987.0 ± 4.5	111 ± 14	141.9 ± 2.2	0.10313 ± 0.00044	45,659 ± 5,549	10,317 ± 50	10,256 ± 50	146.1 ± 2.3
Paraoir5–3.7 m	−3.7	2,566.9 ± 5.8	677.7 ± 5.6	143.5 ± 3.2	0.06833 ± 0.00020	4,273 ± 36	6,720 ± 29	6,654 ± 29	146.2 ± 3.3
Paraoir5–4.7 m	−4.7	2,954.5 ± 3.8	812.2 ± 8.7	144.9 ± 2.1	0.07459 ± 0.00019	4,479 ± 49	7,346 ± 24	7,280 ± 24	148.0 ± 2.2
Paraoir5–12 m	−12.0	2,754.6 ± 2.9	193.0 ± 8.1	144.0 ± 1.8	0.08551 ± 0.00022	20,152 ± 842	8,470 ± 27	8,409 ± 27	147.5 ± 1.9

Table 1 continued

Sample ID	Depth (m)	^{238}U (ppb)	^{232}Th (ppt)	δ^{234}U measured[a]	$[^{230}Th/^{238}U]$ activity[b]	$[^{230}Th/^{232}Th]$ (ppm)[c]	Age uncorrected	Age (yr BP) corrected[b,d]	$\delta^{234}U_{initial}$ corrected[e]
Paraoir5–13 m	−13.0	3,302.1 ± 4.6	31.4 ± 5.9	143.4 ± 2.1	0.08566 ± 0.00023	148,575 ± 27,664	8,490 ± 29	8,430 ± 29	146.8 ± 2.2

Depth annotated with "−" or "+" sign indicates depth below or above present sea level. Analytical errors are 2σ of the mean

Chemistry was performed during November 2008–March 2009 and instrumental analyses on MC-ICP-MS (Shen et al. 2012)

[a] $\delta^{234}U = \left(\left[^{234}U/^{238}U\right]_{activity} - 1\right) \times 1000$

[b] $\delta^{234}U_{initial}$ corrected was calculated based on ^{230}Th age (T), i.e., $\delta^{234}U_{initial} = \delta^{234}U_{measured} \times e^{\lambda_{234} \times T}$, and T is corrected age

[c] $\left[^{230}Th/^{238}U\right]_{activity} = 1 - e^{-\lambda_{230}T} + \left(\delta^{234}U_{measured}/1000\right)\left[\lambda_{230}/(\lambda_{230} - \lambda_{234})\right]\left(1 - e^{-(\lambda_{230} - \lambda_{234})T}\right)$, where T is the age. Decay constants are 9.1577 × 10^{-6} yr^{-1} for ^{230}Th, 2.8263 × 10^{-6} yr^{-1} for ^{234}U (Cheng et al. 2000), and 1.55125 × 10^{-10} yr^{-1} for ^{238}U (Jaffey et al. 1971)

[d] The degree of detrital ^{230}Th contamination is indicated by the $[^{230}Th/^{232}Th]$ atomic ratio instead of the activity ratio

[e] Age corrections were calculated using an estimated atomic $^{230}Th/^{232}Th$ ratio of 4 ± 4 ppm and then calibrated to 1950 AD. Those are the values estimated from shallow corals with an arbitrarily assumed error of 100 %

Fig. 3 Photographs of cores of the Paraoir reef. (**a**) Algal–coral boundstones, PAR-4, 1–4 m in depth, length of core box = 1 m. (**b**) Coral rubble and bioclastics, PAR-2, depth 2.65–3 m and 3.65–4 m

occurs in the lower part of the cores. The representative corals in the facies are *Acropora* and *Heliopora*.

The volcanic and bioclastic facies consists of tuffaceous matter and bioclastic grains in argillaceous matrix. The facies belongs to the Plio–Pleistocene Rosario Formation that underlies the Holocene reef limestones. Cores PAR-1, 3, and 5 did not reach the Rosario Formation because of the loss of circulation during drilling operation.

Coral ages

The lithological columns and coral ^{230}Th ages (Fig. 4, Table 1) reveal coral ages fall into two distinct groups. Coral ages of PAR-4 and PAR-5, located on the reef margin, range from 10.26 to 6.65 kyr BP, and systematically increase with depth. Corals of PAR-1, PAR-2, and PAR-3, located in the backreef area, are much younger with ages ranging from 803 to 324 yr BP and do not systematically decrease in ages upward. Samples from the surface near PAR-1 (PAR-1A, 1B, and 1C) and the rampart were dated at 634–755 yr BP and 759 ± 11 yr BP, respectively, consistent to the ages of cores in the backreef area.

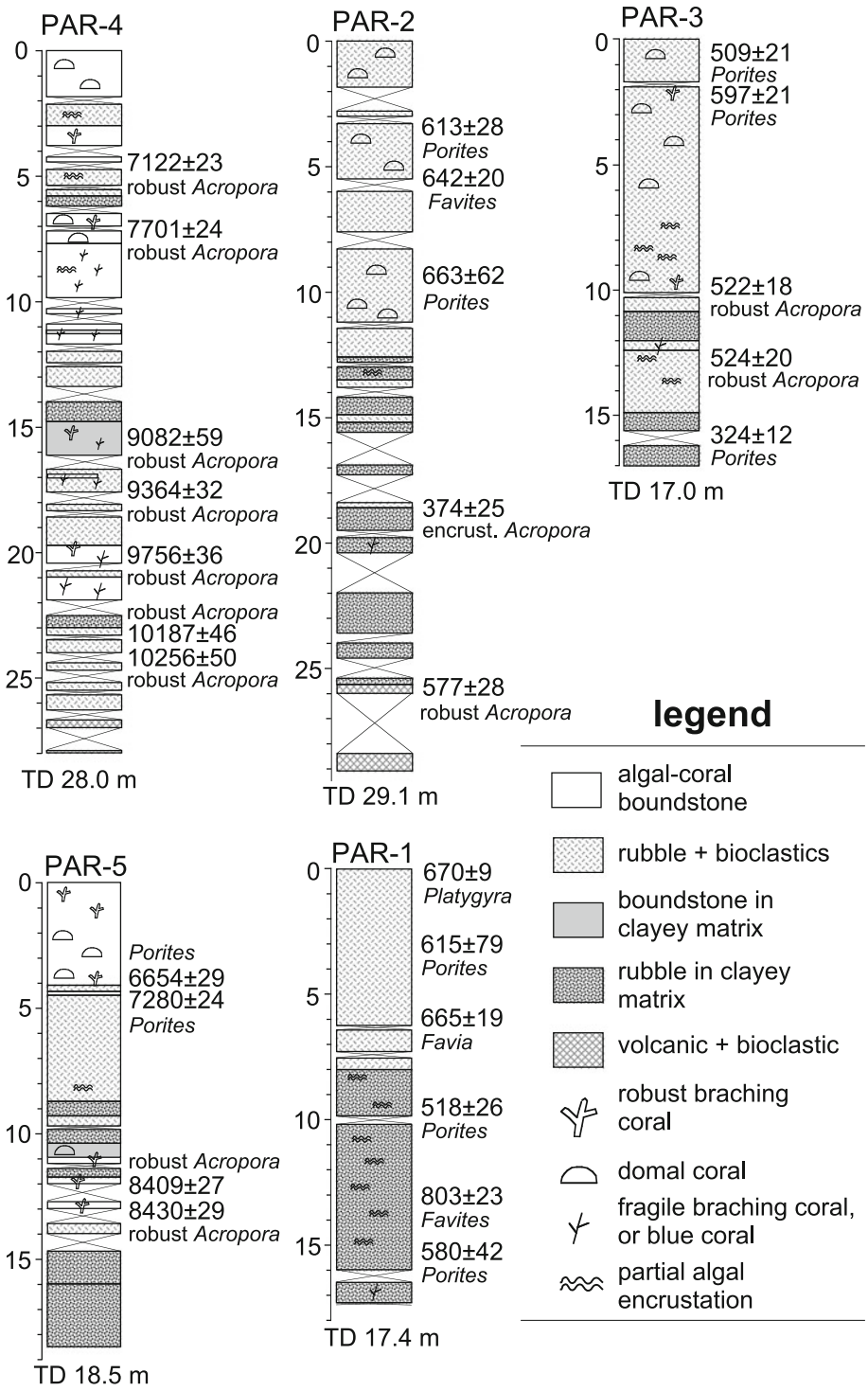

Fig. 4 Lithocolumn with coral ^{230}Th ages of the Paraoir cores. Depths are below the ground surface. The elevation of PAR-1, PAR-2, and PAR-3 is 0.4 m above MSL. PAR-4 and PAR-5 are at near MSL

Historical archives

A chronology of typhoons in Philippines from records made by Spanish missionaries was compiled by Selga (1935). Based on Selga's report, several devastating tropical cyclones in west Luzon from the seventeenth to early nineteenth century were identified (Ribera et al. 2008), including ones on August 5, 1639, October 5, 1649, October 23, 1767, and October 22, 1831, respectively.

Catalogue of earthquakes and probable tsunamis or seiches on the basis of Spanish archives was provided by Saderra Masó (1910) and Repetti (1946). Wiegel (1980) reviewed the historical records of tsunamis and listed several tsunamis in the seventeenth to nineteenth century

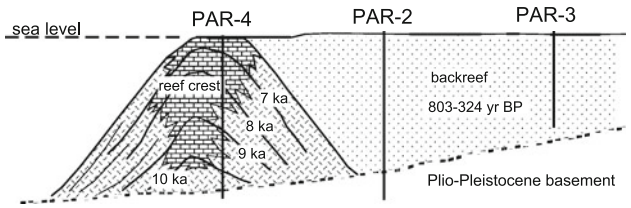

Fig. 5 Schematic profile of facies geometry with time lines reconstructed from the Paraoir cores PAR-4, PAR-2, and PAR-3

that might have affected Luzon: a tsunami struck Cagayan (N. Luzon) in 1627; a seiche in Pasig River, Manila, on 1645; a tsunami hit S and SW Luzon on 1677; a probable tsunami hit N. Luzon in 1744; a probable tsunami hit Subic Bay area in 1852; a seiche in the Manila Bay in 1863. None of those historical records indicated any places near the study site were among areas affected by the tsunami events. Two tsunamis in the early twentieth century did strike northwestern coast of Luzon, one on May 6, 1924 and another on February 14, 1934 (Repetti 1946; Wiegel 1980).

Tsunami simulation

The 1924 earthquake-induced tsunami was reported to be insignificant (Repetti 1946; Wiegel 1980). The 1934 earthquake (Mw = 7.9) (Fig. 1a), stronger than the 1924 one (Mw = 7), was recorded to have a tsunami on the nearby coast of Luzon at San Esteban of Ilocos Sur (Repetti 1946), about 65 km north of Paraoir. However, no quantified report was available for this induced tsunami. Okal et al. (2011) relocated the event using the arrival times published by the ISS and the method of Wysession et al. (1991), and the solution converges to 17.47 N, 119.09 W. They also inverted the momentum tensor of the source and found that the focal mechanism was able to be interpreted as an oblique thrust ($\lambda = 53°$) on a plane striking $\varphi = 338°$ and dipping $\delta = 46°$ to the north. Our simulation result shows that the maximum wave height at the study site is less than 0.4 m (Fig. 6).

Discussion

Backreef infilling and EWE

The facies anatomy and history of Paraoir reef (Fig. 5) suggest that reef development occurred in two stages. First, the reef started at least as early as 10.26 kyr BP on a bioclastic substrate along the margin as indicated by the location of PAR-4 and PAR-5 (Figs. 4, 5). The reef accreted vertically till about 6.65 kyr BP when it probably reached the paleosea level. A small lagoon existed behind the reef throughout its growth. At the second stage, the lagoon was filled and reef flat built by sediments of about 300–800 years in age.

Holocene reefs throughout the world's tropical ocean have shown variable growth patterns. The Paraoir reef anatomy (Fig. 5) can be characterized as a "reef with shallow lagoon" (Kennedy and Woodroffe 2002), or as an "unbalanced aggrading" reef using the classification of Montaggioni (2005). Holocene backreef infilling in the Pacific Ocean typically started sometime around 7–4 kyr BP when the rate of sea level rise slowed down (Smith et al. 1998; Cabioch et al. 1999; Yamano et al. 2001; Kayanne et al. 2002; Kennedy and Woodroffe 2000; Purdy and Gischler 2005).

The Paraoir reef formed from 10.26 to 6.65 kyr BP, while the sediments in the moat were dated to be 818–324 yr BP (Figs. 4, 5). The ages indicate that the moat was filled about 6 kyr after the reef stopped growing. Although unbalanced aggrading models are common in Holocene reefs in the Indo-Pacific region, such an extended age gap between the reef growth and backreef deposition is very rare if not unique. Although backreef deposition started when sea level stabilized after 6000 yr BP, backreef zones typically remain as "open bucket" as backreef filling is generally minimal (Purdy and Gischler 2005). The Paraoir data provided a new style of reef-flat formation in which it started much later than other cases but completed within at most a few hundred years.

Core PAR-5 ended almost 10 m short of PAR-5; as a consequence, the time of reef initiation at the site of PAR-5 is unknown. It is possible that the reef built progressively from the south to north, or in reverse. Nevertheless, the oldest coral in the backreef zone is near 6000 years younger the youngest coral in the reef framework. There is no doubt that the backreef sedimentation lag far behind reef growth; even the reef might have progressed laterally from the south to north or in reverse.

Coral ages and lithofacies suggest that the Paraoir backreef infilling resulted from an EWE. First, corals from core PAR-1, 2, and 3 are completely disordered in depth–age correlation (Figs. 4, 5). Second, the three cores from the backreef area consist primarily of coral rubble without any in situ framework. These two features suggest that those corals did not grow in situ but were totally detrital and reworked. The sedimentation rates (over 20 m within several 100 years) are too rapid to be caused by normal depositional processes, such as tides, normal-weather waves, or longshore currents. The lack of an age–depth relationship suggests that those sediments did not accumulate by a gradual process but through a single EWE that occurred after 324 yr BP.

If there were two or more such extreme events, the lower part of the backreef sediments would be generally

older than the upper part, and younger corals would be absent in the lower part. For example, corals of 500–800 yr BP occurred in the lower while 300–800 yr BP in the upper part. But the observation does not support this scenario (Fig. 4). A single event best explains the age–depth pattern of corals in the three cores. It is described in the section "Lithology" that the surface of backreef sediments is already lithified as hard rock and has been leveled by wave cut for about 100–150 m in width perpendicular to coast. Lithification and wave erosion are gradual processes and need time to occur. Therefore, the EWE likely happened sometime closer to 324 yr BP than the recent few decades.

Tropical cyclone possibility

Among the possible origins for such an EWE, only a tsunami or tropical cyclone could cause catastrophic waves capable of erosion and deposition of such large amounts of coral rubble onshore (Ball et al. 1967; Baines et al. 1974; Nott and Hayne 2001; Fabricius et al. 2008; Frohlich et al. 2009; Scheffers et al. 2009; Goff et al. 2011). Tsunami and storm deposits share many similar features. Some sedimentary fabrics or structures were proposed to be diagnostic of tsunami deposits but only occur in siliciclastic deposits (Kortekaas and Dawson 2007) and generally, only a particular characteristic may be present in any specific tsunami deposit (Dominey-Howes 2007). In coral reef setting, the most important criterion is reef boulder transportation (Goto et al. 2010). For example, a tsunami can move reef-limestone boulders of several tens even more than 100 tons (metric) in weight to depositional positions 10–20 m above sea level and several hundreds meters inland, or boulders of several tons for 500 m to over 1,000 m (Kelletat et al. 2004; Kortekaas and Dawson 2007; Frohlich et al. 2009; Scheffers et al. 2009; Goto et al. 2010).

The Ishigaki Island of Japan may also be invaded by both tsunami and tropical cyclones just like this case, thus can serve as an analogue of the Philippines. At Ibaruma reef and Shiraho reef of Ishigaki Island, the reef-rock boulders deposition by severe storms are mostly <5 tons in weight and occur 50–200 m away from the reef edge, while those deposited by tsunamis average often several tens of tons in weight and scatter widely between 390 and 1,290 m from the edge (Goto et al. 2010). The Ishigaki reefs offer an opportunity to document that the transportation of large reef boulders (>10 tons) can be used as a diagnosis to identify tsunami deposits in areas where both tsunami and tropical cyclones occur. No such large boulders were observed at Paraoir coast. In addition, the inland margin of the pebble- to cobble-sized backreef deposits, exposed on the banks of the fishpond (Fig. 1), is only about 350 m from the reef edge, compared to 390–1,290 m for much heavier boulders (Goto et al. 2010). Therefore, the Paraoir backreef deposition seems to be more likely caused by a severe storm.

A coral rubble in the northern part of reef flat (Fig. 1) was dated to be 818 ± 11 yr BP. Similar ramparts caused by severe storms occurred on several Pacific reef islands (Scoffin 1993). The two observations of (1) the coral rubble rampart is located in the north of the reef flat and (2) the present moat opens to the north both suggest that the storm deposits were most likely brought into their present position through the open in the north (Fig. 1). It is mentioned earlier in the text that modern coral reefs occur extensively along the La Union coasts (Aliño 2003). These reefs might well be the source of the sediments now deposited in backreef zone of Paraoir.

Previous studies have suggested that a single storm can deposit coral rubble up to several meters thick (Baines et al. 1974; Scoffin 1993; Nott and Hayne 2001; Rasser and Riegl 2002). The volume of storm deposits at Paraoir should be in the order of one million cubic meters based on the area and thickness of storm-generated backreef deposit observed on surface and in cores (Figs. 1, 4). An estimated volume of 1.4×10^6 m^3 backreef deposit was generated by Hurricane Bebe on Funafuti in 1972 (Baines et al. 1974). The tropical cyclone that hits Paraoir had caused similar impact as Bebe did to Funafuti. The wind speed of Bebe was greater than 50 m s^{-1} and storm surge about 3–4 m high (Baines et al. 1974), comparable to category 5 typhoons. Typhoons of category 5 in the western Pacific are hardly rare. During a 20-year period from 1970 to 1989, a total of 7 super typhoons (wind speed ≥238 km h^{-1} or 65 m s^{-1}) struck the Philippine Islands (Shoemaker 1991). Typhoon-generated waves with significant wave height of several meters are common in western Pacific or South China Sea (Ou et al. 2002; Chu and Cheng 2008).

The severe cyclone responsible for Paraoir backreef infilling should occur sometime in the seventeenth to nineteenth centuries, based on the age of the youngest fossil coral, 324 ± 12 yr BP. Ribera et al. (2008) identified several devastating tropical cyclones in west Luzon from the seventeenth to early nineteenth century, including ones on August 5, 1639, October 5, 1649, October 23, 1767, and October 22, 1831, respectively. One of these severe cyclones could have caused the backreef infilling at Paraoir. Unfortunately, there was no instrumental record of those typhoons. It is not possible to compare those typhoons to Hurricane Bebe.

Tsunami possibility

A tsunami is another possible agent that caused the abrupt backreef sedimentation at Paraoir. Several lines of reasoning suggest that a tsunami is less likely to be

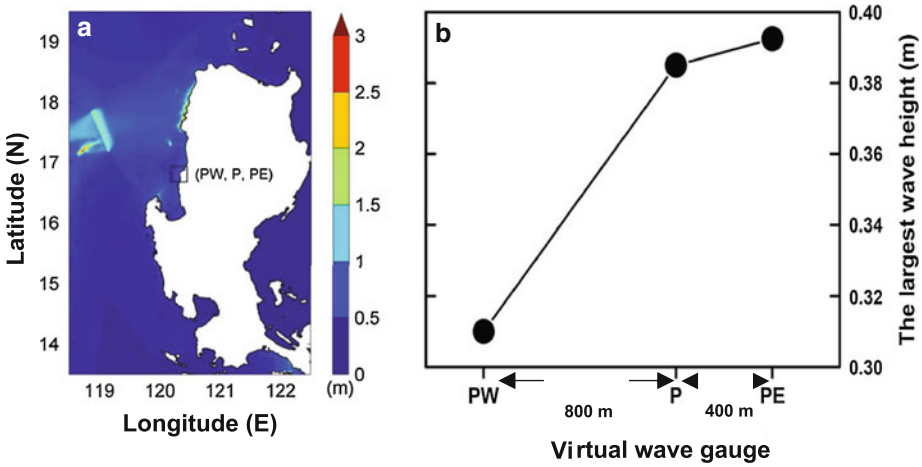

Fig. 6 **a** Simulated tsunamis induced by the 1934 earthquake off Northwestern Luzon. The length and width of the seismogenic zone are 82.6 and 35.9 km, respectively. The magnitude and dislocation are Mw = 7.9 and $D = 2.9$ m. **b** The respective induced largest wave heights at the three virtual wave gauges, *PW*, *P*, and *PE*. Refer to Fig. 1b for the location of three wave gauge sites

responsible for the Paraoir EWE deposition, although we cannot rule out the possibility.

As mentioned earlier, historical records indicated the La Union coast was not affected by the tsunamis in sixteenth–eighteenth centuries. Two tsunamis in the early twentieth century did hit the La Union coast, one in 1924, another in 1934.

The epicenters of the 1627, 1677, 1852, 1863, 1924, and 1934 earthquakes as estimated by Bautista and Oike (2000) are plotted in Fig. 1a, which shows that most of those tsunamigenic earthquakes are not located off the northwest coast of Luzon except the ones of 1924 and 1934. The earthquake on May 6, 1924 (Mw = 7) resulted in tsunami affecting Agno, western Luzon (16.1°N and 119.8°E) with no significant damage (Wiegel 1980). The one on February 14, 1934 (Mw = 7.9) also generated tsunami to the coast of San Esteban, north to the La Union Province (Repetti 1946). This tsunami could also have struck the Paraoir coast. However, our simulation shows that the wave height generated by this earthquake could be only 0.4 m when it reached the Paraoir coast (Fig. 6), seemingly too small to deposit such a large amount of sediments in the backreef zone. This simulation suggests that the Paraoir EWE deposition was probably not caused by a tsunami.

In conclusion, the absolute-dated fossil corals of five cores drilled from a Holocene fringing reef, developing during 6.6–10.3 kyr BP, at Paraoir of Northwestern Luzon show an EWE-induced instant 26-m-thick deposition in an empty moat behind the reef after 324 yr BP. This abrupt backreef infilling was most likely caused by a severe tropical cyclone based on field observations, tsunami simulations, and historic archives. Compared to the Holocene reefs previously reported, the backreef deposition at Paraoir lagged behind by several 1000 years, yet finished abruptly. Our finding provides a new mode of reef-flat development.

Acknowledgments This study was supported by NSC grant 97-2116-M-178-003 and 98-2116-M-178-004 to SYG. ^{230}Th dating at the HISPEC was supported by the NSC and NTU grants 99-2611-M-002-006 and 99-2628-M-002-012, 100-2116-M-002-009, and 102R7625 to CCS. The authors thank the municipal government of Balaoan, La Union, for granting the drilling permit and Don Mariano Marcos Memorial State University for field accommodation. The authors thank Dr. Y. Maeda, Dr. C.F. Dai, and Dr. G.S. Burr for valuable discussions.

References

Aliño PM (2003) Philippine coral reefs through time. Coral Reef Information Network. Philippines and Univ Philippines Mar Sci Inst, p 198

Baines GBK, Beveridge PK, Maragos JE (1974) Storm and island building at Funafuti Atoll, Ellice Islands. Proc 2nd Int Coral Reef Symp 2:485–496

Ball MM, Shinn EA, Stockman KW (1967) The geologic effects of Hurricane Donna in south Florida. J Geol 75:583–597

Bautista MLP, Oike K (2000) Estimation of the magnitudes and epicenters of Philippine historical earthquakes. Tectonophysics 317:137–169

Blanchon P, Jones B, Kalbfleisch W (1997) Anatomy of a fringing reef around Grand Cayman: Storm rubble, not coral framework. J Sediment Res 67:1–16

Braithwaite CJR, Montaggioni LF, Camoin GF, Dalmasso H, Dullo WC, Mangini A (2000) Origins and development of Holocene coral reefs: A revisited model based on reef boreholes in the Seychelles, Indian Ocean. Int J Earth Sci 89:431–445

Cabioch G, Montaggioni LF, Faure G, Ribaud-Laurenti A (1999) Reef coralgal assemblages as recorders of paleobathymetry and sea level changes in the Indo-Pacific province. Quaternary Sci Rev 18:1681–1695

Cheng H, Edwards RL, Hoff J, Gallup CD, Richards DA, Asmersom Y (2000) The half-lives of uranium-234 and thorium-230. Chem Geol 169:17–33

Chu PC, Cheng KF (2008) South China sea wave characteristics during Typhoon Muifa passage in winter 2004. J Oceanogr 64:1–21

Dominey-Howes D (2007) Geological and historical records of tsunami in Australia. Mar Geol 239:99–123

Fabricius KE, De'ath G, Poutinen ML, Done T, Cooper TF, Burgess SC (2008) Disturbance gradients on inshore and offshore coral reefs caused by a severe tropical cyclone. Limnol Oceanogr 53:690–704

Frohlich C, Hornbach MJ, Taylor FW, Shen C-C, Moala A, Morton AE, Kruger J (2009) Huge erratic boulders in Tonga deposited by a prehistoric tsunami. Geology 37:131–134

Goff J, Chagué-Goff C, Dominey-Howes D, McAdoo B, Cronin S, Bonté-Grapetin M, Nichol S, Horrocks M, Cisternas M, Lamarche G, Pelletier B, Jaffe B, Dudley W (2011) Palaeo-tsunamis in the Pacific islands. Earth-Sci Rev 107:141–146

Goto K, Miyagi K, Kawamata H, Imamura F (2010) Discrimination of boulders deposited by tsunami and storm waves at Ishigaki Island, Japan. Mar Geol 269:34–45

Hopley D, Smithers SG, Parnell KE (2007) The geomorphology of the Great Barrier Reef: Development, diversity, and changes. Cambridge University Press, p 532

Hubbard DK (1992) Hurricane-induced sediment transport in open-shelf tropical systems : An example from St. Croix, U.S Virgin Islands. J Sediment Petrol 62:946–960

Jaffey AH, Flynn KF, Glendenin LE, Bentley WC, Essling AM (1971) Precision measurement of half-lives and specific activities of U-235 and U-238. Phys Rev 4:1889–1906

Kayanne H, Yamano H, Randall RH (2002) Holocene sea-level changes and barrier reef formation on an oceanic island, Palau Islands, western Pacific. Sediment Geol 150:47–60

Kelletat D, Scheffers A, Scheffers SR (2004) Holocene tsunami deposits on the Bahaman Islands of Long Island and Eleuthera. Z Geomorphol 48:519–540

Kennedy DM, Woodroffe CD (2000) Holocene lagoonal sedimentation at the latitudinal limits of reef growth, Lord Howe Island, Tasman Sea. Mar Geol 169:287–304

Kennedy DM, Woodroffe CD (2002) Fringing reef growth and morphology: A review. Earth-Sci Rev 57:255–277

Kortekaas S, Dawson AG (2007) Distinguishing tsunami and storm deposits: An example from Martinhal, SW Portugal. Sediment Geol 200:208–221

Liu PLF, Cho YS, Yoon SB, Seo SN (1994) Numerical simulations of the 1960 Chilean tsunami propagation and inundation at Hilo, Hawaii. In: El-Sabh MI (ed) Recent development in tsunami research. Kluwer Academic, Dordrecht, the Netherlands, pp 99–115

Liu PLF, Wang X, Salisbury AJ (2009) Tsunami hazard and early warning system in South China Sea. J Asian Earth Sci 36:2–12

Macintyre IG, Glynn PW, Steneck RS (2001) A classic Caribbean algal ridge, Holandés Cays, Panama: An algal coated storm deposit. Coral Reefs 20:95–105

Maeda Y, Siringan FP (2004) Atlas of Holocene notches and the coral reef terraces of the Philippine Islands (I). National Humanity Activities 8:97–175

Megawati K, Shaw F, Sieh K, Huang Z-H, Wu T-R, Lin Y-N, Tan SK, Pan T-C (2009) Tsunami hazard from the subduction megathrust of the South China Sea: Part I. Source characterization and the resulting tsunami. J Asian Earth Sci 36:13–20

Montaggioni LF (2005) History of Indo-Pacific coral reef systems since the last glaciation: Development patterns and controlling factor. Earth Sci Rev 71:1–75

National Mapping and Resource Information Authority (NAMRIA) (2001) Tide and current tables Philippines 2001. Oceanography Division, Coast and Geodetic Survey, NAMRIA, Manila p 256

Nott J, Hayne M (2001) High frequency of super-cyclones along the Great Barrier Reef over the past 5,000 years. Nature 413:508–512

Okada Y (1986) Surface deformation due to shear and tensile faults in a half-space. Bull Seismol Soc Am 75:1135–1154

Okal EA, Synolakis CE, Kalligeris N (2011) Tsunami simulations for regional sources in the South China and adjoining seas. Pure Appl Geophys 168:1153–1173

Ou SH, Liau JM, Hsu TW, Tzang SY (2002) Simulating typhoon waves by SWAN wave model in coastal waters of Taiwan. Ocean Eng 29:947–971

Purdy EG, Gischler E (2005) The transient nature of the empty bucket model of reef sedimentation. Sediment Geol 175:35–47

Ramos NT, Tsutsuni H (2010) Evidence of large prehistoric offshore earthquakes deduced from uplifted Holocene marine terraces in Pangasinan Province, Luzon Island, Philippines. Tectonophysics 495:145–158

Rasser M, Riegl B (2002) Holocene coral reef rubble and its binding agents. Coral Reefs 21:57–72

Repetti WC (1946) Catalogue of Philippine earthquakes, 1589–1899. Bull Seismol Soc Am 36:133–319

Ribera P, Garcia-Herrera R, Gimeno L (2008) Historical deadly typhoons in the Philippines. Weather 63:194–199

Saderra Masó M (1910) Catalogue of violent and destructive earthquakes in the Philippines 1599–1909. Manila Central Observatory, Weather Bureau, Department of The Interior, p 27

Scheffers SR, Scheffers A, Browne T, Haviser J (2009) Tsunamis, hurricanes, the demise of coral reefs and shifts in prehistoric human populations in the Caribbean. Quaternary Int 195:69–87

Schlager W (1993) Accommodation and supply—a dual control on stratigraphic sequence. Sediment Geol 86:111–136

Scoffin TP (1993) The geological effects of hurricanes on coral reefs and the interpretation of storm deposits. Coral Reefs 12:203–221

Selga M (1935) Charts of remarkable typhoons in the Philippines 1902–1934. Catalogue of typhoons 1348–1934. Manila Weather Bureau, Manila, p 55

Shen C-C, Edwards RL, Cheng H, Dorale JA, Thomas RB, Moran SB, Weinstein SE, Hirschmann M (2002) Uranium and thorium isotopic and concentration measurements by magnetic sector inductively coupled plasma mass spectrometry. Chem Geol 185:165–178

Shen C-C, Cheng H, Edwards RL, Moran SB, Edmonds HN, Hoff JA, Thomas RB (2003) Measurement of attogram quantities of ^{231}Pa in dissolved and particulate fractions of seawater by isotope dilution thermal ionization mass spectroscopy. Anal Chem 75:1075–1079

Shen C-C, Li K-S, Sieh K, Natawidjaja D, Cheng H, Wang X, Edwards RL, Lam DD, Hsieh Y-T, Fan T-Y, Meltzner AJ, Taylor FW, Quinn TM, Chiang H-W, Kilbourne KH (2008) Variation of initial ^{230}Th/^{232}Th and limits of high precision U–Th dating of shallow-water corals. Geochim Cosmochim Acta 72:4201–4223

Shen C-C, Wu C-C, Cheng H, Edwards RL, Hsieh Y-T, Gallet S, Chang C-C, Li T-Y, Lam DD, Kano A, Hori M, Spötl C (2012) High-precision and high-resolution carbonate ^{230}Th dating by MC-ICP-MS with SEM protocols. Geochim Cosmochim Acta 99:71–86

Shoemaker DN (1991) Characteristics of tropical cyclones affecting the Philippine Islands. Naval Oceanography Command Center/ Joint Typhoon Warning Center Technical Note 91–1:1–35

Smith BT, Frankel E, Jell JS (1998) Lagoonal sedimentation and development of Heron Reef, southern Great Barrier Reef Province. In: Camoin CF, Davies PJ (eds) Reefs and carbonate platforms in the Pacific and Indian Oceans, International Association of Sedimentologists Special Publication 27: 281–294

Wang X, Liu PLF (2006) An analysis of 2004 Sumatra earthquake fault plane mechanisms and Indian Ocean tsunami. J Hydraul Res 44:147–154

Wiegel RL (1980) Tsunamis along west coast of Luzon, Philippines. In: Proceedings of the 17th Coastal Engineering Conference, The American Society of Civil Engineers 1:652–671

Wu T-R, Huang H-C (2009) Modeling tsunami hazards from Manila trench to Taiwan. J Asian Earth Sci 36:21–28

Wu T-R, Chen P-F, Tsai W-T, Chen G-Y (2008) Numerical study on tsunami excited by 2006 Pingtung earthquake doublet. Terrestrial, Atmospheric Ocean Sci 19:705–715

Wysession ME, Okal EA, Miller KL (1991) Intraplate seismicity of the Pacific Basin, 1913–1988. Pure Appl Geophys 135: 261–359

Yamano H (2000) Sensitivity of reef flats and reef islands to sea-level change. Proc 9th Int Coral Reef Symp 2:1193–1198

Yamano H, Kayanne H, Yonekura N (2001) Anatomy of a modern coral reef flat: a recorder of storms and uplift in the Late Holocene. J Sediment Res 71:295–304

Yen YT, Ma KF (2011) Source-scaling relationship for M 4.6–8.9 earthquakes, specifically for earthquakes in the collision zone of Taiwan. Bull Seismol Soc Am 101:464–481